

**Universitat de Lleida**

Document downloaded from:

<http://hdl.handle.net/10459.1/60518>

The final publication is available at:

<https://doi.org/10.1111/bjd.15121>

(c) Wiley Online Library, 2016

**Immunohistochemical analysis of T-type calcium channels in  
acquired melanocytic nevi and melanoma**

Maiques O<sup>1†</sup>, Macià A<sup>1†</sup>, Moreno S<sup>2</sup>, Barceló C<sup>1</sup>, Santacana M<sup>3</sup>, Vea A<sup>2</sup>, Herreros J<sup>1</sup>, Gatus S<sup>3</sup>,  
Ortega E<sup>4</sup>, Valls J<sup>5</sup>, Chen BJ<sup>6</sup>, Llobet-Navas D<sup>7</sup>, Matias-Guiu X<sup>3</sup>, Cantí C<sup>1\*</sup>, Marti RM<sup>2\*</sup>

<sup>1</sup>University of Lleida, IRBLleida, Departments of <sup>2</sup>Dermatology, <sup>3</sup>Pathology and Molecular  
Genetics and <sup>4</sup>Oncology, Hospital Universitari Arnau de Vilanova, University of Lleida,  
IRBLleida, <sup>5</sup>Biostatistics Unit, IRBLleida, Lleida, SPAIN. <sup>6</sup>New York Genome Center, New York,  
USA. <sup>7</sup>Institute of Genetic Medicine, Newcastle University, Newcastle upon Tyne, UK.

<sup>†</sup>OM and <sup>†</sup>AM should be considered as first authors.

\*CC and \*RMM should be considered as co-senior authors.

## Abstract

**BACKGROUND AND OBJECTIVES:** Cutaneous malignant melanoma arises from transformed melanocytes *de novo* or from congenital or acquired melanocytic nevi. We have recently reported that T-type  $\text{Ca}^{2+}$  channels (TTCs) are upregulated in human melanoma and play an important role on cell proliferation. The aim of this study was to describe for the first time in formalin-fixed-paraffin-embedded tissue the immunoexpression of TT-Cs in biopsies of normal skin, acquired melanocytic nevi and melanoma, in order to evaluate their role in melanomagenesis and/or tumor progression, their utility as prognostic markers and their possible use in targeted therapies.

**METHODS:** Tissue samples from normal skin, melanocytic nevi and melanoma were subjected to immunohistochemistry for two TT-Cs (Cav3.1, Cav3.2), markers of proliferation (Ki67), cell cycle (Cyclin D1), hypoxia (Glut1), vascularization (CD31) and autophagy (LC3), V600E/BRAF mutation (VE-1) and PTEN. Immunostaining was evaluated by *histoscore*. In silico analysis was used to assess the prognostic value of TT-Cs over-expression.

**RESULTS:** TT-Cs immunoexpression increased gradually from normal skin to common nevi, dysplastic nevi and melanoma samples, but with differences in distribution of both isoforms. Particularly, Cav3.2 expression was significantly higher in metastatic melanoma than in primary melanoma. Statistical correlation showed a lineal interaction between PTEN-loss/ V600E-BRAF/ Cav3.1/ LC3/ Ki67/ Cyclin D1/ Cav3.2 /Glut1. Disease-free survival (DFS) and global survival (OS) correlated inversely with over-expression of Cav3.2. DFS also correlated inversely with over-expression of Cav3.1.

**DISCUSSION:** TT-Cs immunoexpression on melanocytic neoplasms 1) is consistent with our previous *in vitro* studies, 2) appears related to tumor progression, and 3) TT-Cs upregulation can be considered as a prognostic marker using TCGA database. The high expression of Cav3.2 in metastatic melanoma encourages the investigation of the use of TT-Cs blockers in targeted therapies.

Original Article: Translational Research

What's already known about this topic?

An increased expression of voltage gated calcium channels (VGCCs) is a common finding in several neoplasms. We have recently reported that T-type  $\text{Ca}^{2+}$  channels (TT-Cs) are upregulated in human melanoma cells and play an important role in cell proliferation, calcium homeostasis and autophagic flux.

What does this study add?

We describe for the first time in formalin-fixed-paraffin-embedded tissue the immunoexpression of TT-Cs in biopsies of normal skin, acquired melanocytic nevi and melanoma. We have found that TT-Cs immunoexpression increases gradually from normal skin to common nevi, dysplastic nevi and melanoma samples, and that the expression of the Cav3.2 isoform is augmented in metastatic vs. primary melanoma. We also demonstrate a significant correlation between Breslow thickness and TT-Cs expression. In addition, we show a positive correlation between the immunoexpression of Cav3.2 and proliferative/hypoxia markers. Furthermore, we show a positive association between the expression of the Cav3.1 isoform, the autophagy markers and the presence of the BRAF/V600E mutation. These findings open a new venue of research regarding the use of T-type blockers in targeted therapies.

## Introduction

Melanoma is the most dangerous form of skin cancer, and its incidence is steadily increasing worldwide<sup>1,2</sup>. In spite of being the subject of intense laboratory investigations, numerous clinical trials, and the emergence of new and much more effective drugs, the prognosis of metastatic melanoma is still poor<sup>3</sup>.

Ca<sup>2+</sup>-signaling is suspected to play an important role in the development as well as in the viability, survival and motility of cancer cells<sup>4,5</sup>. It is known that external Ca<sup>2+</sup> is needed to induce cell proliferation and cell cycle progression in mammalian cells. Several types of Ca<sup>2+</sup> channels have been described. Among them, voltage-gated calcium channels (VGCCs) are the most highly selective for Ca<sup>2+</sup> ions<sup>6,7</sup>.

VGCCs have been classified by their electrophysiological and pharmacological properties and, more recently, by their amino acid sequence identity. Based on their activation threshold, VGCCs have been classified in two main groups. High Voltage-Activated (HVA) VGCCs are characteristic of excitable cells, such as muscle cells or neurons. HVA VGCCs comprise two subfamilies, Cav1 (L-type VGCCs) and Cav2 (P/Q, N and R-VGCCs types). Low Voltage-Activated (LVA) VGCCs are represented by the 3 isoforms of the Cav3 subfamily (Cav3.1, Cav3.2 and Cav3.3), also called T-type channels (TT-Cs)<sup>8</sup>.

TT-Cs display unique low voltage dependent activation/inactivation and slow deactivation kinetics, and carry depolarizing currents at near resting membrane potentials<sup>9</sup>. Therefore, these channels may play a direct role in regulating Ca<sup>2+</sup> levels especially in non-excitable tissues<sup>10</sup>. Numerous studies have demonstrated that the Ca<sup>2+</sup> influx through VGCCs results in signaling that affects the expression of genes involved in cell proliferation, programmed cell death and apoptosis<sup>11,12</sup>. It has been described that the expression of Cav3.1 and Cav3.2 isoforms increases in many cancerous cell types<sup>13–22</sup>.

Our group has recently reported that TT-Cs are also upregulated in human melanoma and play an important role on melanoma cell proliferation and homeostasis. On the contrary, TT-Cs are absent or expressed at low levels in culture human epidermal melanocytes. Moreover, we have demonstrated that pharmacological blockade or gene silencing of TT-Cs induce apoptosis in melanoma cells, which is preceded by endoplasmic reticulum (ER) stress and inhibition of macroautophagy, that is basally activated in this type of tumor cells<sup>23,24</sup>. Deregulation of autophagy is a common feature in malignancy. Evidence for basal increase of autophagy in melanoma is supported by the immunohistochemical detection of LC3-II<sup>25–29</sup> and by electron microscopy studies<sup>30</sup>. In particular, recent studies have demonstrated that melanomas harboring mutant BRAFV600E display an increased basal autophagic rate<sup>31</sup>.

Most of our previous work was done employing melanoma cell lines, cultured human epidermal melanocytes, and a few human melanoma biopsies in which the expression of TT-Cs was studied by RT-PCR. In the present study, we have analyzed the expression of TT-Cs at the protein level in a range series of of formalin-fixed paraffin-embedded (FFPE) biopsies of normal skin, acquired common and dysplastic melanocytic nevi, and primary and metastatic melanoma tumors, in order to evaluate their role in melanomagenesis and/or tumor progression, and their utility as prognostic markers. In addition, we have correlated the expression of the distinct TT-C isoforms with proliferative, cell cycle, autophagy, and hypoxia tissue markers, as well as common mutations V600E/BRAF and PTEN.

**Material and Methods**

**1. Case selection**

The series included the following FFPE tissue samples: 1) 21 biopsies of normal skin and 62 of melanoma tumors (40 primary and 22 metastatic) which were included in three TMA (supplementary table 1); 2) 80 melanocytic nevi [60 common acquired melanocytic nevi (20 junctional, 20 compound and 20 intradermal) and 20 dysplastic nevi] which were studied in full sections in order not to miss de junctional component. Breslow thickness of the different primary melanoma subtypes is recorded in supplementary table 2.

All tumor samples were obtained from Hospital Arnau de Vilanova, Lleida. The tumors were classified following the most recent WHO criteria. The study was approved by the local ethical committee, and a specific informed consent was used. A tissue arrayer device (Beecher Instrument, Silver Spring, MD) was used to construct the TMA. Two selected cylinders (1 mm in diameter) from 2 different areas were included in each case.

**2. Immunohistochemical study**

FFPE samples were subjected to immunohistochemistry (IHC) with specific antibodies in front of two TT-Cs isoforms (Cav3.1, Cav3.2), Ki-67, Cyclin D1, Glut1, CD31, LC3, V600E/BRAF and PTEN. Optimal IHC conditions and procedures for each antibody are listed in table 1. Since reliable antibodies were not commercially available, specific novel Cav3.1 and Cav3.2 antibodies were designed by AntibodyBCN (Barcelona, Spain) against the following peptides: QRRPTSWLDEQRRHSI for Cav3.1 and FTQDVRHGDRWDPTRP for Cav3.2. Rabbits were immunized with the mentioned peptides and raised antibodies were affinity-purified. Specificity of antibodies was tested with appropriate positive and negative controls.

IHC staining was graded semiquantitatively by considering the percentage and intensity of the staining. A histological score (Hs) was obtained from each sample and values ranged from 0 (no immunoreaction) to 300 (maximum immunoreactivity). The score was obtained by applying the following formula,  $Hs = 1 \times (\% \text{ light staining}) + 2 \times (\% \text{ moderate staining}) + 3 \times (\% \text{ strong staining})$ . CD31 and GLUT1 were scored as previously described for membrane markers employing a scale 0 (nul expression) to 3 (strong complete membranous staining)<sup>32</sup>.

**3. Statistical analysis**

For the statistical analysis, means and SD from Hs were calculated to report relative differences in immunoexpression levels between all groups included in Table 1. Levels of immunoexpression of the different group of samples were compared by Kruskal-Wallis test with Dunn's Multiple Comparison Test. A trend test, using a linear model, was employed to evaluate the progression in the immunoexpression levels in normal skin, acquired common nevi, dysplastic nevi, primary melanoma and metastatic melanoma tissue, using this order. Second, Mann-Whitney test was performed to assess whether immunoexpression was similar according to Breslow thickness ( $\leq 1\text{mm}$  vs  $>1\text{mm}$ ). Third, Kruskal-Wallis test with Dunn's Multiple Comparison Test was performed to study differences in the expression of TT-C isoforms between the different clinicopathological primary melanoma subtypes. Fourth, Pearson correlation tests were performed to find significant relationships among the biomarkers. Fifth, optimal threshold in each biomarker was generated by hazar-ratios, and Kaplan-Meier estimates were computed to evaluate both disease free-survival (DFS) and overall survival (OS) by log-rank test to assess significance between survivals curves.

We have carried out a bioinformatics analysis in order to investigate whether TT-Cs are associated with survival in melanoma patients using The Cancer Genome Atlas (TCGA) database (<http://www.cbioportal.org/>; Skin Cutaneous Melanoma) (n = 471 patients)<sup>33,34</sup>. Over-expression of Cav3.1 and Cav3.2 were categorized using RNA Z score cutoff  $\geq 2.0$ . DFS and

OS were obtained as mentioned previously. All analyses were obtained using R statistical software version 3.01 (R Foundation, Vienna, Austria), and statistical significance was set at .05.

## Results

1. Immunohistochemical expression of TT-C isoforms in normal skin, nevi and primary and metastatic melanoma.

IHC analysis of TT-C isoform Cav3.1 and Cav3.2 were positive in all FFPE samples and displayed relevant differences regarding the distribution of both isoforms ( $p < 0.0001$  and  $< 0.0001$ , respectively). Mean, SD and range of Hs were calculated (supplementary table 3) and all possible comparisons were evaluated in order to obtain significant differences (supplementary table 4) by Kruskal-Wallis test with Post Hoc Dunn's Multiple Comparison Test.

On the one hand, Cav3.1 was higher expressed in all malignant melanoma (metastatic and primary) and dysplastic nevi samples (Hs mean: 44.44, 41.86 and 38.5, respectively). Significant differences were found in the following pairs: metastatic melanoma vs normal skin; metastatic melanoma vs acquired common nevi; primary melanoma vs acquired common nevi; dysplastic nevi vs acquired common nevi (Figure 1A).

On the other hand, metastatic melanoma displayed the highest Cav3.2 immunoexpression levels (Hs mean: 220), being significantly different from all other groups (primary melanoma, dysplastic nevi, acquired common nevi and normal skin). Primary melanomas displayed the second highest expression levels of Cav3.2 (Hs mean: 125.16), a value that was significantly higher when compared to that from normal skin. Despite no significant differences were observed in Cav3.2 distribution among both nevi subtypes, a significant higher expression of Cav3.2 in the whole group of nevi vs normal skin was detected (Figure 1B).

A trend of progressively increased expression of TT-Cs from normal skin to metastatic melanoma was significant for both TT-Cs ( $p < 0.0001$ ), (Table 5).

2. Correlation between Breslow thickness and TT-Cs expression in primary melanoma

As Breslow thickness is the most important clinicopathological prognostic factor of primary melanoma, we tried to correlate this parameter with TT-Cs expression. As shown in supplementary table 5 and Figure 2 our data demonstrated a significant correlation between Breslow thickness and Cav3.1 and Cav3.2 expression ( $p < 0.00001$  for both TT-C isoforms). Mean Cav3.1 and Cav3.2 expression (Hs mean: 48.33 and 160.0, respectively) were higher in the group of primary melanoma tumors with Breslow thickness  $> 1$  mm than in the group of tumors with Breslow thickness  $\leq 1$  mm (Hs mean: 33.68 and 83.42, respectively).

3. Expression of TT-C isoforms between the different clinicopathological primary melanoma subtypes

The presence of Cav3.1 and Cav3.2 isoforms in the main four clinicopathological primary melanoma subtypes [SSMM (superficial spreading malignant melanoma), NM (nodular melanoma), ALM (acral lentiginous melanoma) and LMM (lentigo maligna melanoma)] was also studied (supplementary table 6). Mean Cav3.1 immunoexpression was low-moderate in all subtypes and the histoscore did not show global significant differences between them ( $p = 0.07$ ) (Figure 3A). However, mean Cav3.2 immunoexpression was differentially distributed among primary melanoma subtypes ( $p < 0.00001$ ) (supplementary table 7). Cav3.2 immunostaining was strong in NM and ALM (Hs means: 212.22 and 198.33 respectively), apparently according to

their high Breslow thickness, and low-moderate in SSMM according to their variable Breslow thickness (Hs mean: 67.17), with higher expression in very thick SSMM (Figure 3B). However, even the thickest SSMM group (Breslow >4 mm, Hs mean: 105.6) did not reach the high Cav3.2 Hs values of the remainder subtypes. Of note, LMM showed strong Cav3.2 immunoexpression in spite of the very low Breslow thickness of all specimens (supplementary table 2).

4. Correlation between the immunoexpression of TT-Cs and the other biomarkers in melanoma samples

Levels of immunoexpression of both TT-Cs and of all antigens listed in Table 1 were subjected to a statistical correlation analysis in all melanoma samples (primary and metastatic). Significant correlations by Pearson test were obtained between some of them, showing a cluster of linear interactions between partial or complete PTEN loss/ V600E-BRAF/ Cav3.1/ LC3/ Cyclin D1/ Ki67/ Cav3.2/ Glut1. We observed a positive correlation between partial or complete PTEN loss and the presence of the V600E/BRAF mutant protein (p=0.00041). Importantly, this common mutation in melanoma (50-60% of cases) correlated with the expression of Cav3.1 (p=0.0009). Likewise, the expression of this channel isoform was linked to the expression of LC3, an important protein during the autophagic process. In our samples, the levels of LC3 also correlated with the levels of nuclear Cyclin D1 (p=0.01). In turn, nuclear Cyclin D1 showed a positive correlation with Ki67, a marker of proliferation. Finally, Cav3.2 positively correlated with Ki67 (p=0.03) and Glut1 (p=0.003), indicating that the expression of this channel isoform is enhanced in hypoxic and proliferative environments. (Figure 4).

5. Survival studies: Lack of prognostic statistical significance of TT-Cs immunoexpression on disease free survival (DFS) and overall survival (OS) in our series.

Among the 39 patients with a primary tumor, 17 experienced a relapse (39.53%) and 13 died (30.23%). Median DFS and OS were 26.33 months and 51.6 months, respectively. Median follow up was 29.10 months.

Statistical univariate analysis looking for clinicopathological parameters and immunohistochemical biomarkers of primary tumors influencing DFS and OS was done. Clinicopathological variables analyzed were Breslow thickness and 2010 American Joint Committee on Cancer (AJCC) stages. All biomarkers employed in the present study (Cav3.1 Cav3.2, Ki67, Cyclin D1, Glut1, CD31, LC3, V600E/BRAF and PTEN) were included as variables. Log-rank test analysis demonstrated that DFS and OS correlated inversely in a statistically significant way with high AJCC staging (DFS p=0.00006; OS p=0.002), high Breslow thickness (best cutoff 4 mm) (DFS p=0.00003; OS p=0.0001), partial or complete PTEN loss (DFS p<0,00001; OS p=0.0004) and high Ki67 expression (DFS p=0.01; OS p=0.02). Low Cyclin D1 levels correlated with poor OS (DFS p=0.24; OS p=0.02). Cav3.1 or Cav3.2 isoform Hs did not show a statistical impact on survival (Figure 5).

6. Survival studies: in silico analysis of the impact of TT-Cs expression at the RNA level on melanoma prognosis

Due to the lack of prognostic statistical significance of TT-Cs immunoexpression in our series, we studied the impact of TT-Cs upregulation at the RNA level on DFS and OS in the mentioned database (<http://www.cbioportal.org/>). Samples were followed up to 360 months. Although shorter times of follow-up were considered (supplementary Figure 1), highest statistical



significance was observed in 360 months for both TT-Cs. From a total of 398 cases, only 4 cases presented upregulation of Cav3.1 (Figure 5F). Nonetheless, a significant reduction was observed for DFS ( $p=0.026$ ), but OS reduction was no significant ( $p=0.16$ ). In contrast, the Cav3.2 RNA levels were upregulated in 17 and 21 cases from a total of 386 and 439 cases for DFS and OS, respectively. The upregulation of Cav3.2 is strongly associated to a poor outcome represented by significant decreases in DFS and OS (Figure 5G) ( $p=0.012$  and  $0.007$ , respectively).

For Peer Review

Discussion

Malignant melanoma is one of the most life-threatening cutaneous neoplasms. Therefore, investigation about molecules involved in melanoma pathogenesis and progression, which could be used as prognostic markers and/or targets of new therapeutic strategies, is required. It is currently known that cutaneous melanoma may arise on normal skin or on a previous congenital or acquired melanocytic nevus<sup>35,36</sup>. However, the Clark model for melanoma progression, in which melanoma develops from benign melanocytic nevus *via* dysplastic nevus<sup>37,38</sup>, is a useful model to analyse on human specimens the role of potentially relevant molecular targets.

Our group has recently reported that TT-Cs are expressed in melanoma cell lines and metastatic melanoma frozen samples. These channels mediate constitutive Ca<sup>2+</sup> influx in melanoma cells and can be efficiently blocked by pharmacological drugs or silenced at the gene level. Both strategies lead to the apoptotic death of the cultured melanoma cells through ER stress and autophagy inhibition<sup>23,24</sup>.

Taking into account our previous findings, we decided to evaluate the immunoexpression of Cav3.1 and Cav3.2 on a series of human samples which contained the spectrum of melanocytes on normal skin, common acquired melanocytic nevi, dysplastic nevi, primary melanoma tumours with diverse Breslow thickness and metastatic melanoma, using made-to-order antibodies. Consistently with our previous work, Cav3.1 and Cav3.2 proteins were expressed at higher levels in melanoma cells compared to epidermal melanocytes, especially the expression of Cav3.2 in metastatic tumors. Moreover, TT-C immunoexpression increased gradually from melanocytes of normal skin to common nevi, dysplastic nevi, primary melanoma and metastatic melanoma specimens. This progressive increase sustained our hypothesis about the upregulation of TT-Cs during melanoma progression. This was further supported by the observation that the expression of both isoforms was higher in thick (Breslow >1 mm) compared to thin (Breslow ≤ 1 mm) primary tumours.

Regarding the immunostaining of TT-Cs isoforms among the different clinicopathological primary melanoma subtypes, we did not observe differences in relationship to Cav3.1. In contrast, the expression of Cav3.2 showed statistical differences depending on the melanoma subtypes. Overall, Cav3.2 immunostaining was stronger in melanomas with high mean Breslow thickness (NM, ALM) and moderate in tumors with variable Breslow thickness (SSMM). Nevertheless, although very thick SSMM (Breslow >4 mm) showed higher Cav3.2 immunexpression than less thick SSMM tumors (Breslow ≤4mm), differences were not significant. Also, the group of LMM, which included four *in situ* (Breslow =0) and two thin tumors with a mean Breslow of 0.25 mm, displayed a strong Cav3.2 immunostaining. As a matter of fact, the pathogenesis for LMM is quite distinctive and differs from pathogenesis of SSMM, developing on chronically exposed skin of elderly people, usually with a long-lasting radial growth phase and particular histopathological, molecular and genetic features<sup>39</sup>. Since our series included a relatively small number of this LMM subtype (6 cases), in comparison with a majority of SSMM tumors (21 cases), but only 4 SSMM with Breslow >4 mm, broader studies will be necessary to confirm this finding.

Our previous *in vitro* findings indicated that the expression of TT-Cs in melanoma cells is modulated under hypoxic conditions, play a role in melanoma viability and proliferation<sup>24</sup> and that their inhibition results in a blockade of basal macroautophagy (constitutively activated in melanoma cells)<sup>23</sup>. Thus, we decided to check the correlation between the immunoexpression of both TT-C isoforms and proliferation (Ki67), cell cycle (Cyclin D1), hypoxia (Glut1), vascularization (CD31) and autophagy (LC3) biomarkers. In addition, since autophagy has been described to be high in BRAF mutant melanoma<sup>40</sup>, we also tested melanoma samples

employing the currently commercially available VE1 antibody for the immunoexpression of V600E/BRAF mutated protein<sup>41</sup> and the frequently concomitant downregulation of the tumor suppressor protein PTEN<sup>42</sup>. In the current work, Cav3.1 immunoexpression nicely correlated with the LC3 autophagy biomarker and with the presence of the V600E/BRAF mutation which, in turn, was associated with PTEN downregulation as described in the previously mentioned melanoma molecular studies<sup>42</sup>. On the other hand, Cav3.2 expression was closely related to the hypoxia marker Glut1 and the proliferation marker Ki67. Transcriptional upregulation of specific TT-C isoforms by hypoxia has been previously reported in proliferating cells, and found to be mediated by hypoxia inducible factors<sup>43-45</sup>. Furthermore, the level of Ki67 immunostaining was associated with Cyclin D1 expression which, in turn, correlated with LC3, completing the cluster of linear interactions. In summary, our data supports the idea that increased autophagic flux and TT-Cs expression can be regarded as two mechanisms of cell survival inside a tumor with a high proliferation index in a hypoxic environment.

Finally, since we have shown that TT-C expression was related to tumour progression and to adverse prognostic markers of primary tumours such as high Breslow thickness and cell proliferation biomarkers, we checked if it could be also employed as a prognostic factor. In fact, Pera and co-workers have recently shown that high levels of Cav3.2 (measured by RT-qPCR) were associated with poor outcome in patients with estrogen receptor positive breast cancers, whereas, in patients with HER2-positive breast cancers, high Cav3.2 levels were associated to a better OS after chemotherapy<sup>46</sup>. Although Cav3.1 or Cav3.2 histoscores on primary tumors did not show an impact on the prognosis (OS and DFS) of our patients (n=39) (data not shown), we decided to perform a bioinformatics analysis from a larger number of patients. To this end we searched TCGA database through cBioPortal<sup>33,34</sup> an obtained significant, negative associations between the overexpression of Cav3.1 and OS, and between the over-expression of Cav3.2 and OS/DFS. Thus, high levels of TT-Cs are related to bad prognosis, especially for Cav3.2, consistently with a role for these channels in tumor progression/metastasis. Otherwise, classical clinicopathological and immunohistochemical prognostic variables such as high Breslow thickness, advanced AJCC staging and high Ki67 expression were associated with short DFS and poor OS in our sample series, as expected. PTEN downregulation was also identified as a negative predictor for DFS and OS as previously shown<sup>47</sup>. Intriguingly, high Cyclin D1 values were associated with better OS, differing from some other studies on melanoma<sup>48,49</sup> and other neoplasms<sup>50</sup>. Yet, others claimed that Cyclin D1 immunoexpression levels lacked prognostic value in melanoma<sup>51</sup> or even correlated with longer OS in breast cancer patients<sup>52</sup>. Although nuclear expression of cycling D1 is useful to evaluate cell proliferation<sup>53,54</sup>, these discrepancies could be explained by recent reports of new functions of Cyclin D1 that go beyond its classical role in cell cycle and tumorigenesis<sup>55</sup>.

In summary, here we describe for the first time the immunoexpression of TT-C isoforms in a series of formalin-fixed / paraffin embedded tissue samples of human acquired melanocytic nevi and melanoma. We have found that the expression of Cav3.1 and Cav3.2 in normal skin and benign and malignant melanocytic neoplasms is in line with our previous *in vitro* studies in which TT-C transcript levels were studied<sup>56,57</sup>, and appears related to tumour progression. Furthermore, the high expression of Cav3.2 in metastatic vs primary melanoma and its association to proliferative and hypoxia markers, on one hand, and the positive correlation between Cav3.1, autophagy markers and BRAF/V600E mutation on the other, opens a new venue of research regarding the use of T-type blockers in targeted therapies.

1  
2  
3  
4  
5  
6  
7  
8  
9  
10  
11  
12  
13  
14  
15  
16  
17  
18  
19  
20  
21  
22  
23  
24  
25  
26  
27  
28  
29  
30  
31  
32  
33  
34  
35  
36  
37  
38  
39  
40  
41  
42  
43  
44  
45  
46  
47  
48  
49  
50  
51  
52  
53  
54  
55  
56  
57  
58  
59  
60

**Acknowledgements**

Supported by grants from ISCIII (FIS-PI1200260 to RMM, FIS-PI1301980 to JH and RETICS-RD12/0036/0013 to XMG), from Fundació la Marató de TV3 (FMTV 201331-31 to RMM), from Generalitat de Catalunya (2014/SGR138 to XMG) and cofinanced by FEDER “Una manera de hacer Europa”. OM and CB hold a predoctoral fellowship from University of Lleida and SM a predoctoral fellowship from IRBLleida/Diputació de Lleida. Tumour samples were obtained with the support of Xarxa de Bancs de Tumors de Catalunya sponsored by Pla Director d'Oncologia de Catalunya (XBTC) and IRBLleida Biobank (B.0000682) and PLATAFORMA BIOBANCOS (PT13/0010/0014)

For Peer Review

## References

- 1 Thompson JF, Scolyer RA, Kefford RF. Cutaneous melanoma. In: *Lancet*. England, 2005; 687–701.
- 2 Markovic SN, Erickson LA, Rao RD, *et al*. Malignant melanoma in the 21st century, part 1: epidemiology, risk factors, screening, prevention, and diagnosis. In: *Mayo Clin Proc*. United States, 2007; 364–80.
- 3 Hao M, Song F, Du X, *et al*. Advances in targeted therapy for unresectable melanoma: new drugs and combinations. *Cancer Lett* 2015; **359**:1–8.
- 4 Cox JL, Lancaster T, Carlson CG. Changes in the motility of B16F10 melanoma cells induced by alterations in resting calcium influx. *Melanoma Res* 2002; **12**:211–9.
- 5 Glass-Marmor L, Penso J, Beitner R. Ca<sup>2+</sup>-induced changes in energy metabolism and viability of melanoma cells. *Br J Cancer* 1999; **81**:219–24.
- 6 Capiod T. The need for calcium channels in cell proliferation. In: *Recent Pat Anticancer Drug Discov*. United Arab Emirates, 2013; 4–17.
- 7 Macià A, Herreros J, Martí RM, Cantí C. Calcium channel expression and applicability as targeted therapies in melanoma. *Biomed Res Int* 2015; **2015**:587135.
- 8 Perez-Reyes E. Molecular physiology of low-voltage-activated t-type calcium channels. *Physiol Rev* 2003; **83**:117–61.
- 9 Taylor JT, Zeng XB, Pottle JE, *et al*. Calcium signaling and T-type calcium channels in cancer cell cycling. *World J Gastroenterol* 2008; **14**:4984–91.
- 10 Crunelli V, Toth TI, Cope DW, *et al*. The 'window' T-type calcium current in brain dynamics of different behavioural states. In: *J Physiol*. England, 2005; 121–9.
- 11 Nicotera P, Orrenius S. The role of calcium in apoptosis. In: *Cell Calcium*. Scotland, 1998; 173–80.
- 12 Spitzer NC, Gu X, Olson E. Action potentials, calcium transients and the control of differentiation of excitable cells. *Curr Opin Neurobiol* 1994; **4**:70–7.
- 13 Taylor JT, Huang L, Pottle JE, *et al*. Selective blockade of T-type Ca<sup>2+</sup> channels suppresses human breast cancer cell proliferation. *Cancer Lett* 2008; **267**:116–24.
- 14 Leuranguer V, Bourinet E, Lory P, Nargeot J. Antisense depletion of beta-subunits fails to affect T-type calcium channels properties in a neuroblastoma cell line.

*Neuropharmacology* 1998; **37**:701–8.

15 Hirooka K, Bertolesi GE, Kelly MEM, *et al.* T-Type calcium channel alpha1G and alpha1H subunits in human retinoblastoma cells and their loss after differentiation. *J Neurophysiol* 2002; **88**:196–205.

16 Latour I, Louw DF, Beedle AM, *et al.* Expression of T-type calcium channel splice variants in human glioma. *Glia* 2004; **48**:112–9.

17 Mariot P, Vanoverberghe K, Lalevee N, *et al.* Overexpression of an alpha 1H (Cav3.2) T-type calcium channel during neuroendocrine differentiation of human prostate cancer cells. *J Biol Chem* 2002; **277**:10824–33.

18 Lu F, Chen H, Zhou C, *et al.* T-type Ca<sup>2+</sup> channel expression in human esophageal carcinomas: a functional role in proliferation. *Cell Calcium* 2008; **43**:49–58.

19 Toyota M, Ho C, Ohe-Toyota M, *et al.* Inactivation of CACNA1G, a T-type calcium channel gene, by aberrant methylation of its 5' CpG island in human tumors. *Cancer Res* 1999; **59**:4535–41.

20 Shen L, Ahuja N, Shen Y, *et al.* DNA methylation and environmental exposures in human hepatocellular carcinoma. *J Natl Cancer Inst* 2002; **94**:755–61.

21 Li W, Zhang S-L, Wang N, *et al.* Blockade of T-type Ca(2+) channels inhibits human ovarian cancer cell proliferation. *Cancer Invest* 2011; **29**:339–46.

22 Ueki T, Toyota M, Sohn T, *et al.* Hypermethylation of multiple genes in pancreatic adenocarcinoma. *Cancer Res* 2000; **60**:1835–9.

23 Das A, Pushparaj C, Herreros J, *et al.* T-type calcium channel blockers inhibit autophagy and promote apoptosis of malignant melanoma cells. *Pigment Cell Melanoma Res* 2013; **26**:874–85.

24 Das A, Pushparaj C, Bahi N, *et al.* Functional expression of voltage-gated calcium channels in human melanoma. *Pigment Cell Melanoma Res* 2012; **25**:200–12.

25 Hersey P, Zhang XD. Adaptation to ER stress as a driver of malignancy and resistance to therapy in human melanoma. *Pigment Cell Melanoma Res* 2008; **21**:358–67.

26 Lazova R, Camp RL, Klump V, *et al.* Punctate LC3B expression is a common feature of solid tumors and associated with proliferation, metastasis, and poor outcome. *Clin Cancer Res* 2012; **18**:370–9.

- 27 Lazova R, Klump V, Pawelek J. Autophagy in cutaneous malignant melanoma. *J Cutan Pathol* 2010; **37**:256–68.
- 28 Lebovitz CB, Bortnik SB, Gorski SM. Here, there be dragons: charting autophagy-related alterations in human tumors. *Clin Cancer Res* 2012; **18**:1214–26.
- 29 Miracco C, Cevenini G, Franchi A, *et al.* Beclin 1 and LC3 autophagic gene expression in cutaneous melanocytic lesions. *Hum Pathol* 2010; **41**:503–12.
- 30 Ma X-H, Piao S, Wang D, *et al.* Measurements of tumor cell autophagy predict invasiveness, resistance to chemotherapy, and survival in melanoma. *Clin Cancer Res* 2011; **17**:3478–89.
- 31 Corazzari M, Rapino F, Ciccocanti F, *et al.* Oncogenic BRAF induces chronic ER stress condition resulting in increased basal autophagy and apoptotic resistance of cutaneous melanoma. *Cell Death Differ* 2015; **22**:946–58.
- 32 Wolff AC, Hammond MEH, Hicks DG, *et al.* Recommendations for human epidermal growth factor receptor 2 testing in breast cancer: American Society of Clinical Oncology/College of American Pathologists clinical practice guideline update. *J Clin Oncol* 2013; **31**:3997–4013.
- 33 Cerami E, Gao J, Dogrusoz U, *et al.* The cBio cancer genomics portal: an open platform for exploring multidimensional cancer genomics data. *Cancer Discov* 2012; **2**:401–4.
- 34 Gao J, Aksoy BA, Dogrusoz U, *et al.* Integrative analysis of complex cancer genomics and clinical profiles using the cBioPortal. *Sci Signal* 2013; **6**:pl1.
- 35 Takata M, Murata H, Saida T. Molecular pathogenesis of malignant melanoma: a different perspective from the studies of melanocytic nevus and acral melanoma. *Pigment Cell Melanoma Res* 2010; **23**:64–71.
- 36 Weatherhead SC, Haniffa M, Lawrence CM. Melanomas arising from naevi and de novo melanomas--does origin matter? In: *Br J Dermatol*. England, 2007; 72–6.
- 37 Clark WH, Elder DE, Guerry D, *et al.* A study of tumor progression: the precursor lesions of superficial spreading and nodular melanoma. *Hum Pathol* 1984; **15**:1147–65.
- 38 Miller AJ, Mihm MC. Melanoma. *N Engl J Med* 2006; **355**:51–65.
- 39 Kraft S, Granter SR. Molecular pathology of skin neoplasms of the head and neck. *Arch Pathol Lab Med* 2014; **138**:759–87.



40 Maddodi N, Huang W, Havighurst T, *et al.* Induction of autophagy and inhibition of melanoma growth in vitro and in vivo by hyperactivation of oncogenic BRAF. *J Invest Dermatol* 2010; **130**:1657–67.

41 Capper D, Preusser M, Habel A, *et al.* Assessment of BRAF V600E mutation status by immunohistochemistry with a mutation-specific monoclonal antibody. *Acta Neuropathol* 2011; **122**:11–9.

42 Griewank KG, Scolyer RA, Thompson JF, *et al.* Genetic alterations and personalized medicine in melanoma: progress and future prospects. *J Natl Cancer Inst* 2014; **106**:djt435.

43 Del Toro R, Levitsky KL, López-Barneo J, Chiara MD. Induction of T-type calcium channel gene expression by chronic hypoxia. *J Biol Chem* 2003; **278**:22316–24.

44 Carabelli V, Marcantoni A, Comunanza V, *et al.* Chronic hypoxia up-regulates  $\alpha 1H$  T-type channels and low-threshold catecholamine secretion in rat chromaffin cells. *J Physiol* 2007; **584**:149–65.

45 Sellak H, Zhou C, Liu B, *et al.* Transcriptional regulation of  $\alpha 1H$  T-type calcium channel under hypoxia. *Am J Physiol Cell Physiol* 2014; **307**:C648–56.

46 Pera E, Kaemmerer E, Milevskiy MJG, *et al.* The voltage gated  $Ca(2+)$ -channel Cav3.2 and therapeutic responses in breast cancer. *Cancer Cell Int* 2016; **16**:24.

47 Meyer S, Fuchs TJ, Bosserhoff AK, *et al.* A seven-marker signature and clinical outcome in malignant melanoma: a large-scale tissue-microarray study with two independent patient cohorts. *PLoS One* 2012; **7**:e38222.

48 Heenen M, Laporte M. [Molecular markers associated to prognosis of melanoma]. *Ann dermatologie vénéréologie* 2003; **130**:1025–31.

49 Vízkeleti L, Ecsedi S, Rákossy Z, *et al.* The role of CCND1 alterations during the progression of cutaneous malignant melanoma. *Tumour Biol* 2012; **33**:2189–99.

50 Xu S, Gu G, Ni Q, *et al.* The expression of AEG-1 and Cyclin D1 in human bladder urothelial carcinoma and their clinicopathological significance. *Int J Clin Exp Med* 2015; **8**:21222–8.

51 Oba J, Nakahara T, Abe T, *et al.* Expression of c-Kit, p-ERK and cyclin D1 in malignant melanoma: an immunohistochemical study and analysis of prognostic value. *J Dermatol*



- 1  
2  
3 *Sci* 2011; **62**:116–23.
- 4  
5 52 Reis-Filho JS, Savage K, Lambros MBK, *et al.* Cyclin D1 protein overexpression and  
6 CCND1 amplification in breast carcinomas: an immunohistochemical and chromogenic  
7 in situ hybridisation analysis. *Mod Pathol* 2006; **19**:999–1009.
- 8  
9  
10 53 Baldin V, Lukas J, Marcote MJ, *et al.* Cyclin D1 is a nuclear protein required for cell cycle  
11 progression in G1. *Genes Dev* 1993; **7**:812–21.
- 12  
13  
14 54 Kim JK, Diehl JA. Nuclear cyclin D1: an oncogenic driver in human cancer. *J Cell Physiol*  
15 2009; **220**:292–6.
- 16  
17  
18 55 Pestell RG. New roles of cyclin D1. *Am J Pathol* 2013; **183**:3–9.
- 19  
20 56 Das A, Pushparaj C, Herreros J, *et al.* T-type calcium channel blockers inhibit autophagy  
21 and promote apoptosis of malignant melanoma cells. *Pigment Cell Melanoma Res* 2013;  
22 **26**:874–85.
- 23  
24  
25 57 Das A, Pushparaj C, Bahí N, *et al.* Functional expression of voltage-gated calcium  
26 channels in human melanoma. *Pigment Cell Melanoma Res* 2012; **25**:200–12.
- 27  
28  
29  
30  
31  
32  
33  
34  
35  
36  
37  
38  
39  
40  
41  
42  
43  
44  
45  
46  
47  
48  
49  
50  
51  
52  
53  
54  
55  
56  
57  
58  
59  
60

**Legend for Figures**

**Figure 1. TT-Cs immunostaining in several type of samples.** 1. Cav3.1 (A) and Cav3.2 (B) mean  $\pm$  SD expression Hs in normal skin (only epidermal melanocytes)\*, acquired common nevi, dysplastic nevi, primary melanoma and metastatic melanoma. 2. Representative images for Cav3.1 expression in normal skin (C), acquired common nevi (D), dysplastic nevi (E) primary melanoma (F) and metastatic melanoma (G). Representative images for Cav3.2 expression in normal skin (H), acquired common nevi (I), dysplastic nevi (J) primary melanoma (K) and metastatic melanoma (L). Arrows show low/negative staining in epidermal melanocytes of normal skin. Hs mean were analyzed by Kruskal-Wallis test with Dunn's Multiple Comparison Test. \*p<0,05; \*\* p<0,01; \*\*\* p<0,001.

**Figure 2. Differential immunoexpression of Cav3.1 (A) and Cav3.2 (B) according to Breslow thickness ( $\leq$  1mm vs  $>$  1mm) in primary melanoma tumors.** Hs mean  $\pm$  SD were analyzed by Mann-Whitney test. \*p<0,05; \*\* p<0,01; \*\*\* p<0,001.

**Figure 3. Differential expression of Cav3.1 (A) and Cav3.2 (B) according primary melanoma subtype.** SSMM (superficial spreading malignant melanoma); NM (nodular melanoma); ALM (acral lentiginous melanoma); LMM (lentigo.maligna melanoma). SSMM have been also divided according Breslow thickness. Hs mean  $\pm$  SD was analyzed by Kruskal-Wallis test with Dunn's Multiple Comparison post hoc Test. \*p<0,05; \*\* p<0,01; \*\*\* p<0,001.

**Figure 4. Statistically significant linear correlations between expression of immunohistochemical biomarkers.** Pearson correlation tests of Hs were performed to find significant relationships among all the biomarkers employed in this study. A. Diagram of statistically significant correlations: low PTEN Hs - high BRAF/V600E Hs (p=0.00041), high BRAF/V600E Hs - high Cav3.1 Hs (p=0.0009), high Cav3.1 Hs - high LC3 Hs (p=0.01), high LC3 Hs - high CyclinD1 Hs (p=0.01), high Cyclin D1 Hs - high Ki67 Hs (p=0.003), high Ki67 Hs - high Cav3.2 Hs (p=0.03) and high Cav3.2 Hs - high Glut1 Hs (p=0.003). B. Immunostaining of biomarkers showing a statistically significant correlation in the same melanoma specimen (PTEN-BRAF/V600E (B,C), BRAF/V600E-Cav3.1 (D,E), Cav3.1-LC3 (F,G), LC3-Cyclin D1 (H,I), Cyclin D1-Ki67 (J,K), Ki67-Cav3.2 (L,M), Cav3.2-Glut1 (N,O).

**Figure 5. Disease free survival (DFS) and Overall survival (OS) curves according statistically significant prognostic clinico-pathologic variables and biomarkers.** AJCC stages\* (A), Breslow thickness (B), PTEN (C), Ki67 (D), Cyclin D1 (E) immunoexpression. Cav3.1(F) and Cav3.2(G) curves generated using TCGA database (<http://www.cbioportal.org/Skin Cutaneous Melanoma>). Altered=overexpression, Z-score  $\geq 2$ . \*Risk groups are based on 2010 AJCC staging and grouped as: In situ (0), low risk (IA/IB), moderate risk (IIA), high risk (IIB/IIC-III), distant metastasis (IV). Hs cut-off values are included in brackets [ ]

**Supplementary figure 1. In silico analysis of the impact of Cav3.2 expression at the RNA level on melanoma prognosis at several times.** A) 60 B) 120 and C) 240 months follow up. Z-score  $\geq 2$ .

**TABLE 1. Information about the procedures and optimized analytical variables in each antibody employed in the study**

Antigen	Staining Pattern	Staining evaluation	Clone	Pretreatment / Detection platform *	Dilution	Source
Cav 3.1	Membranous and cytoplasmic	Membranous and cytoplasmic	Polyclonal	PT Link Low 95°C 20 min / EnvisionFlex	1/150	Antibody BCN (Barcelona, Spain)
Cav 3.2	Membranous, cytoplasmic and nuclear occasionally	Membranous and cytoplasmic	Polyclonal	PT Link High 95°C 20 min / EnvisionFlex	1/200	Antibody BCN (Barcelona, Spain)
Ki67**	Nuclear	Nuclear	MIB-1	PT Link Low 95°C 20 min / EnvisionFlex	RTU***	Dako (Glostrup, Denmark)
Cyclin D1**	Nuclear and cytoplasmic	Nuclear	EP12	PT Link High 95°C 20 min / EnvisionFlex	RTU	Dako (Glostrup, Denmark)
Glut1	Membranous	Membranous	SPM498	PT Link Low 95°C 20 min / EnvisionFlex	1/100	Thermo Fisher Scientific (Waltham, USA)
CD31	Membranous	Membranous	JC70A	PT Link High 95°C 20 min / EnvisionFlex	RTU	Dako (Glostrup, Denmark)
LC3	Cytoplasmic	Cytoplasmic	Polyclonal	PT Link Low 95°C 20 min / EnvisionFlex	1/200	Novus (Littleton, USA)
BRAF/V600E	Cytoplasmic	Cytoplasmic	VE1	Ventana conditions	RTU	Ventana (Tucson, USA)
PTEN	Nuclear and cytoplasmic	Cytoplasmic	6H2.1	PT Link High 95°C 20 min / EnvisionFlex	1/100	Dako (Glostrup, Denmark)

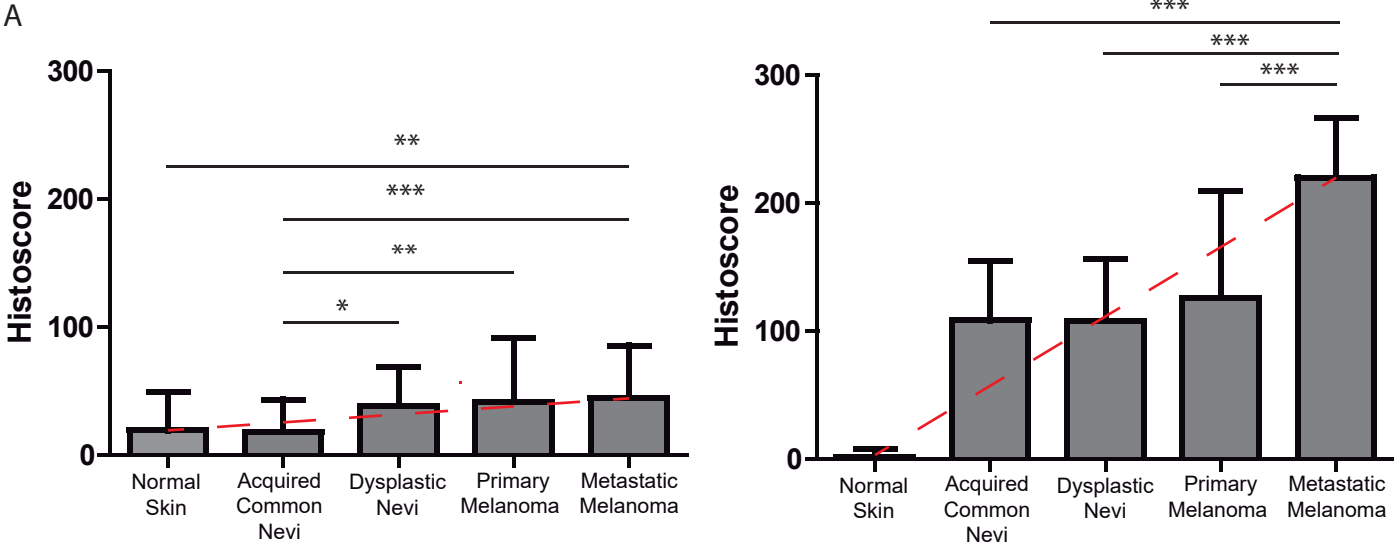
Antigen detected, staining pattern, staining evaluation, clone, optimized protocol (pretreatment conditions, platform employed for detection, dilution) and source of the antibodies.

\* Pretreatment / Detection platform

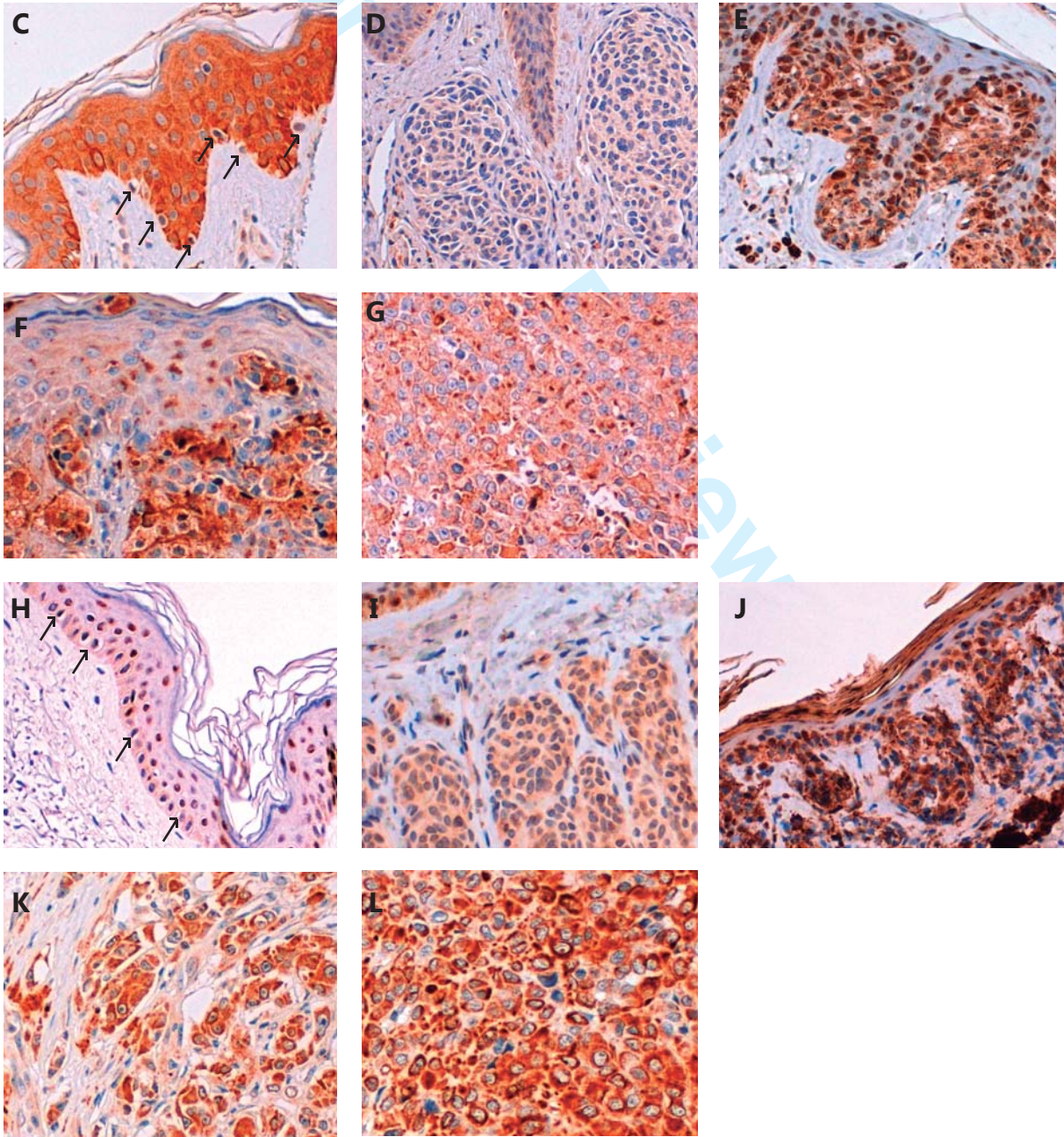
- Epitope retrieval in the PreTreatment Module, PT-LINK (Dako, Glostrup, Denmark)
- EnVision FLEX Detection Kit (Dako, Glostrup, Denmark) using diaminobenzidine chromogen as a substrate.
- BRAF/V600E detection was performed using Ventana platform (Tucson, Arizona, USA).

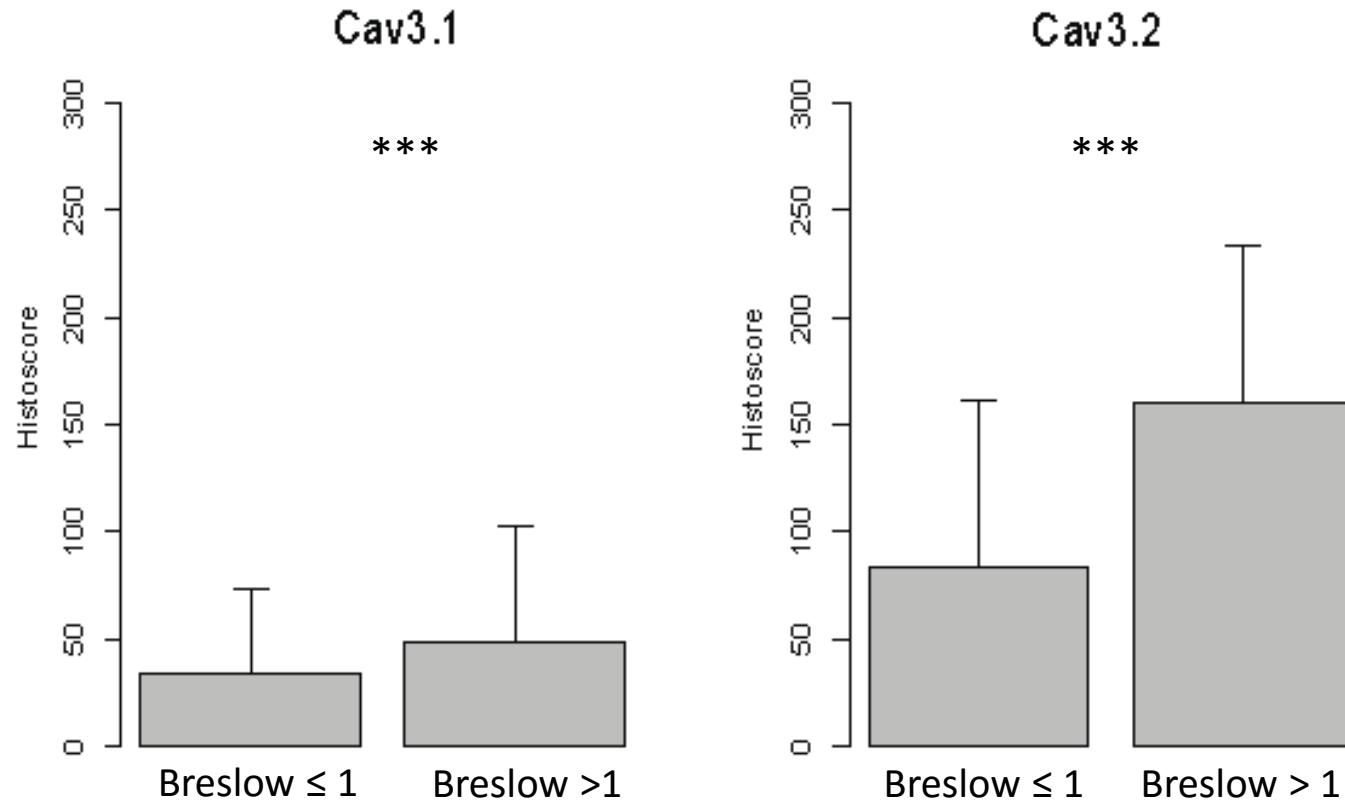
\*\*Proliferation and cell cycle markers (Ki67 & Cyclin D1) were not evaluated in *in situ* melanoma (Breslow 0) due to the difficulty of discerning between proliferating *in situ* melanoma cells and proliferating keratinocytes of the epidermal basal layer, especially when lentiginous epidermal hyperplasia was present.

\*\*\*RTU: Ready to use



	Cav.3.1	Cav.3.2
Kruskal-Wallis	<0.0001	<0.0001
Trend-Test	<0.0001	<0.0001

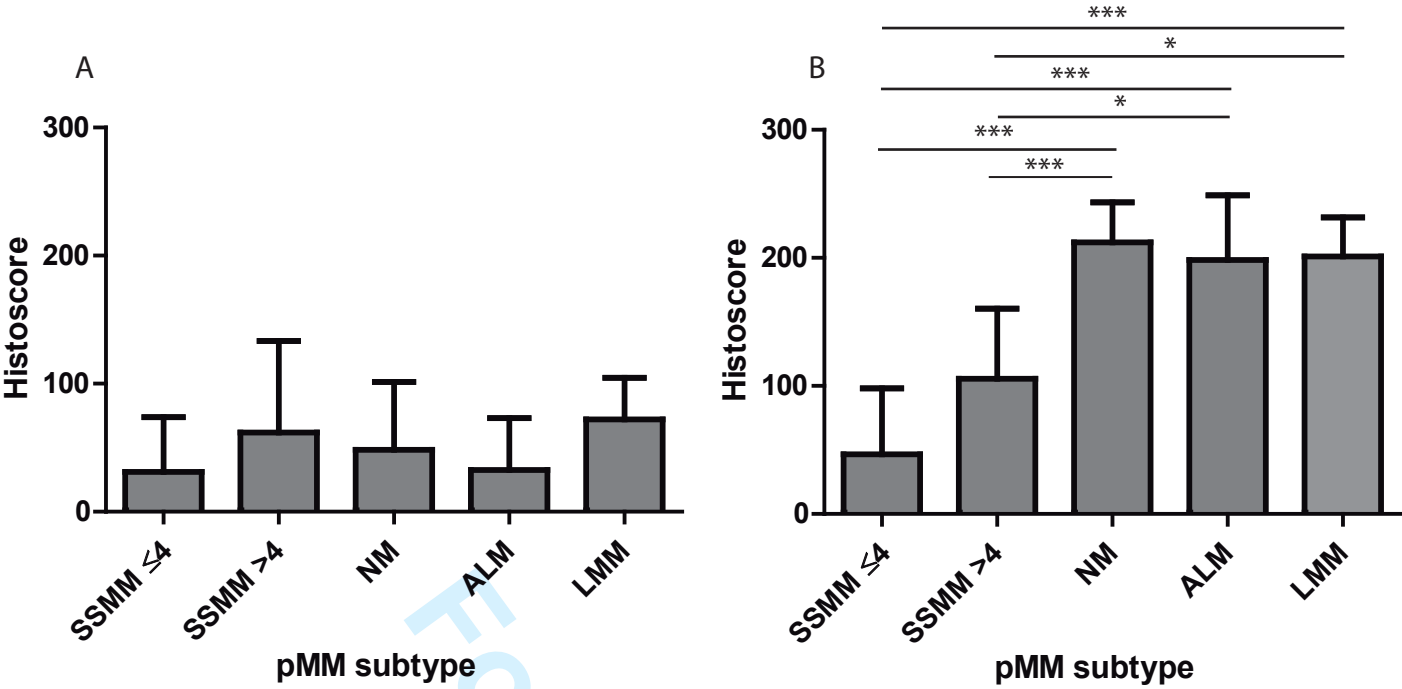






Cav 3.1

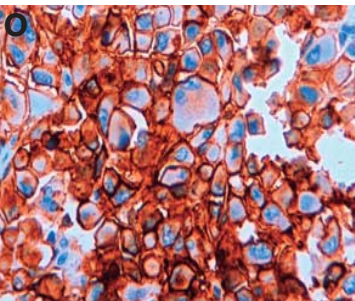
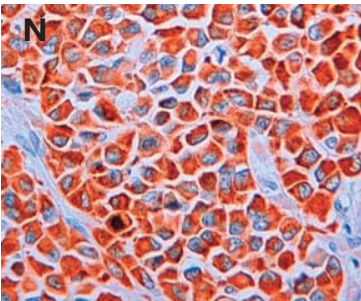
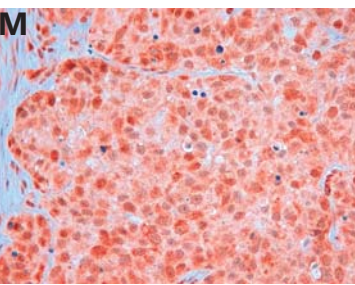
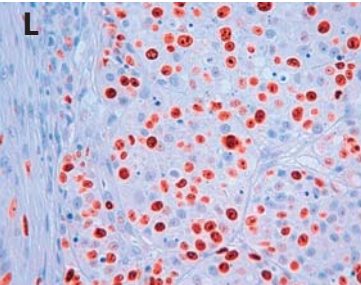
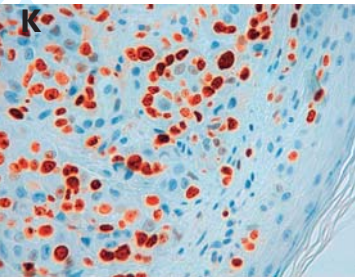
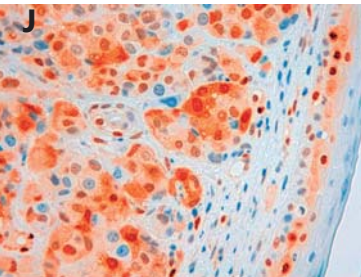
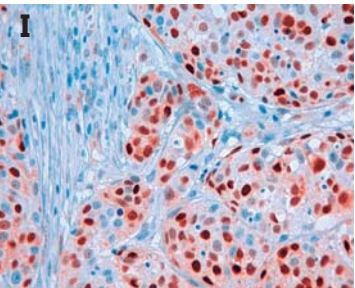
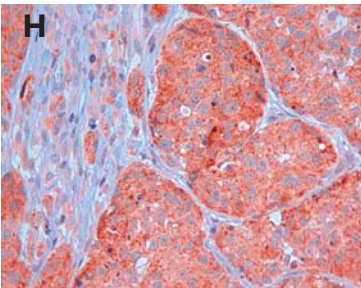
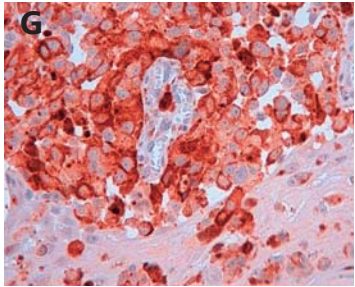
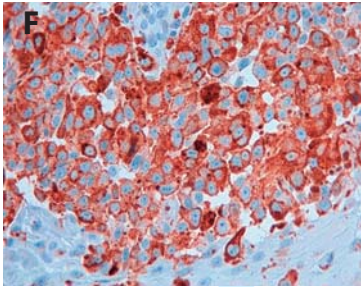
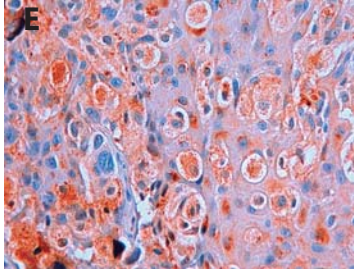
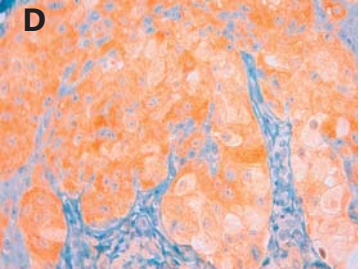
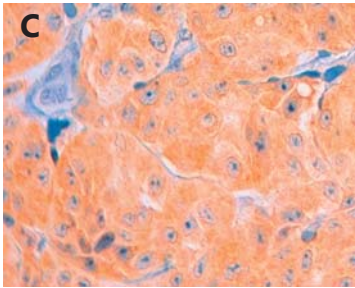
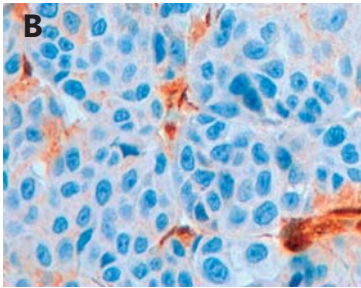
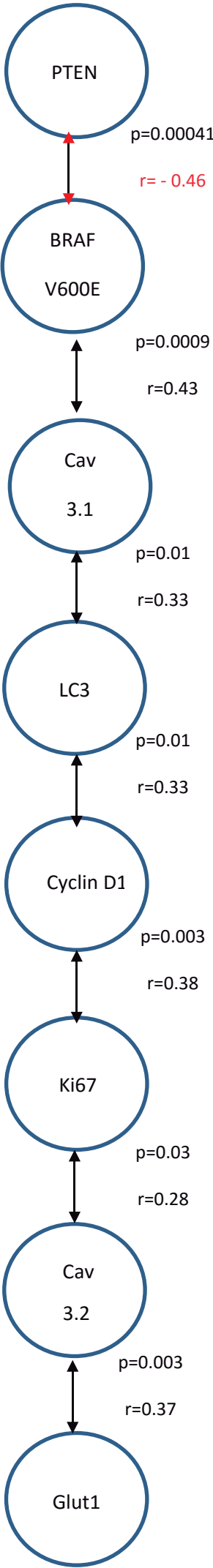
Cav 3.2

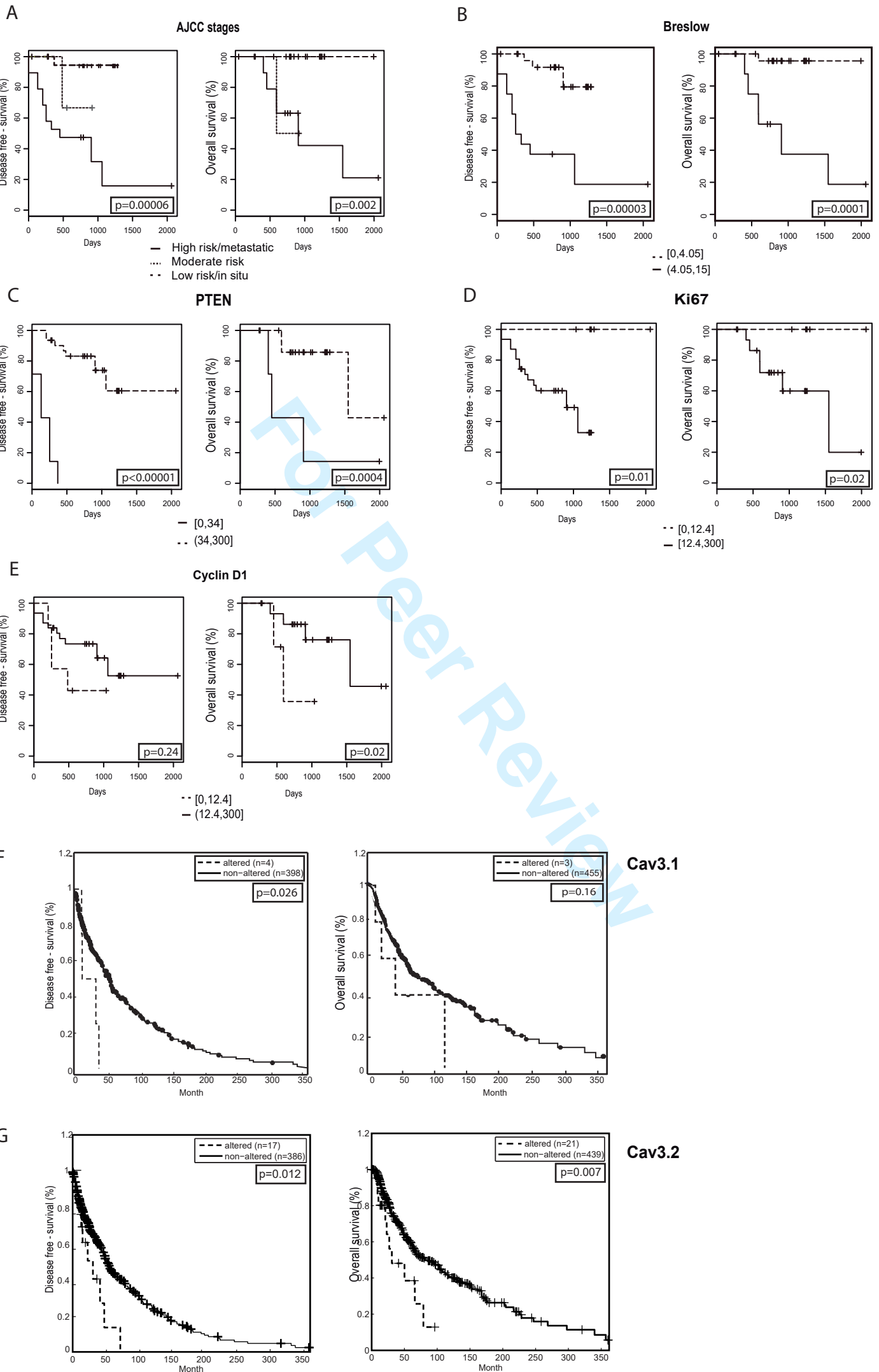


	Cav.3.1	Cav.3.2
Kruskal-Wallis	0.07	<0.0001

**A**

1  
2  
3  
4  
5  
6  
7  
8  
9  
10  
11  
12  
13  
14  
15  
16  
17  
18  
19  
20  
21  
22  
23  
24  
25  
26  
27  
28  
29  
30  
31  
32  
33  
34  
35  
36  
37  
38  
39  
40  
41  
42  
43  
44  
45  
46  
47  
48  
49  
50  
51  
52  
53  
54  
55  
56  
57  
58  
59  
60







**SUPPLEMENTARY TABLE 1. Clinicopathological data of primary and metastatic melanoma cases.**

N	Type of sample	Age	Gender	Localization	Subtype	Breslow (mm)	AJCC stage
1	Primary Tumor	66	F	Lower Limb	SSMM	0.90	IA
2		81	F	Trunk	SSMM	13.54	IIC
3		20	F	Lower Limb	SSMM	0.48	IB
4		80	F	Lower Limb	SSMM	1.17	IB
5		87	F	Foot	SSMM	7.30	IIC
6		85	F	Trunk	SSMM	2.77	IIA
7		79	M	Trunk	SSMM	3.65	IIA
8		48	F	Upper Limb	SSMM	0.00	0
9		80	F	Upper Limb	SSMM	0.26	IA
10		46	F	Head and Neck	SSMM	0.62	IA
11		64	F	Lower Limb	SSMM	0.52	IA
12		71	M	Lower Limb	SSMM	5.20	IIIC
13		69	M	Head and Neck	SSMM	0.00	0
14		62	M	Trunk	SSMM	0.82	IA
15		65	M	Trunk	SSMM	0.57	IA
16		37	M	Trunk	SSMM	0.00	0
17		52	F	Upper Limb	SSMM	6.50	IIB
18		65	M	Trunk	SSMM	0.50	IA
19		42	M	Trunk	SSMM	0.52	IA
20		47	F	Lower Limb	SSMM	0.40	IA
21		45	F	Trunk	SSMM	0.00	0
22		55	F	Upper Limb	NM	0.95	IB
23		64	M	Upper Limb	NM	3.88	IIB
24		69	M	Trunk	NM	5.01	IV
25		59	M	Trunk	NM	2.50	IIA
26		62	F	Upper Limb	NM	0.93	IB
27		61	M	Head and Neck	NM	11.00	IIC
28		75	M	Head and Neck	LMM	0.00	0
29		85	M	Head and Neck	LMM	0.00	0
30		84	M	Head and Neck	LMM	0.00	0
31		72	M	Head and Neck	LMM	0.00	0
32		86	F	Lower Limb	LMM	0.61	IA
33		61	M	Head and Neck	LMM	0.86	IA
34		84	M	Foot	ALM	2.70	IIA
35		64	F	Upper Limb	ALM	5.50	IIC
36		91	M	Foot	ALM	10.00	IIB
37		60	F	Foot	ALM	0.00	0
38		67	M	Foot	ALM	4.29	IIC
39		89	F	Upper Limb	ALM	2.70	IIA
40		49	F	Lower Limb	Unclassifiable	Unknown	Unknown
1	Metastasis	87	F	Cutaneous/ SC			
2		63	M	Peritoneum			
3		85	F	Cutaneous/ SC			
4		77	M	Lymph node			
5		77	M	Lymph node			
6		78	F	Cutaneous/ SC			
7		62	M	Lung			
8		75	M	Adrenal			
9		70	M	Lymph node			
10		52	F	Lung			
11		82	F	Cutaneous/ SC			
12		62	M	Lymph node			
13		62	M	Cutaneous/ SC			
14		53	F	Lymph node			
15		69	M	Lymph node			
16		79	F	Parotid			
17		54	M	Soft tissues			
18		54	M	Lymph node			
19		83	F	Cutaneous/ SC			
20		51	F	Lymph Node			
21		45	F	Cutaneous/ SC			
22		46	F	Lymph Node			

1  
2  
3  
4  
5  
6  
7  
8  
9  
10  
11  
12  
13  
14  
15  
16  
17  
18  
19  
20  
21  
22  
23  
24  
25  
26  
27  
28  
29  
30  
31  
32  
33  
34  
35  
36  
37  
38  
39  
40  
41  
42  
43  
44  
45  
46  
47  
48  
49  
50  
51  
52  
53  
54  
55  
56  
57  
58  
59  
60

SSMM: Superficial Spreading Malignant Melanoma, NM: Nodular Melanoma, LMM: Lentigo Maligna Melanoma, ALM: Acral Lentiginous Melanoma. SC: subcutaneous. 2010 AJCC classification.

For Peer Review

**SUPPLEMENTARY TABLE 2. Breslow thickness of primary melanoma subtypes.**

pMM subtype	Breslow thickness (mm)			
	Mean	Median	SD	range
<b>SSMM</b>	2.17	0.57	3.4	0-13.54
<b>SSMM <math>\leq 4</math> mm</b>	0.78	0.52	0.98	0-3.65
<b>SSMM <math>&gt;4</math>mm</b>	8.13	6.9	3.71	5.2-13.54
<b>NM</b>	4.05	3.19	3.77	0.95-11
<b>ALM</b>	4.2	3.5	3.39	0-10
<b>LMM</b>	0.25	0	0.39	0-0.86

pMM (primary melanoma), SSMM (superficial spreading malignant melanoma); NM (nodular melanoma); ALM (acral lentiginous melanoma); LMM (lentigo.malignant melanoma). SD: Standard deviation

**SUPPLEMENTARY TABLE 3. Cav3.1 and Cav 3.2 immunostaining measured by  
histoscore on normal skin, melanocytic nevi and melanoma samples**

	NS	ACMN	DN	pMM	mMM
TT-C isoform	Mean (SD, HsRange)	Mean (SD, HsRange)	Mean (SD, HsRange)	Mean (SD, HsRange)	Mean (SD, HsRange)
Cav3.1 (Hs)	19.29 (28.82, 0-120)	10.83 (19.51, 0-100)	38.5 (30.66, 0-100)	41.86 (48.46, 0-120)	44.44 (39.22, 0-140)
Cav 3.2 (Hs)	1.9 (6.02, 0-20)	108.67 (46.59, 20-210)	108 (48.73, 30-200)	126.16 (83.73, 0-250)	220 (47.19, 60-270)

TT-C (T-type channel); NS (epidermal melanocytes on normal skin); ACMN (acquired common melanocytic nevi); DN (dysplastic nevi); pMM (primary melanoma); mMM (metastatic melanoma). SD: Standard deviation, HsRange: Histological Score Range

**SUPPLEMENTARY TABLE 4. Statistical comparison of mean Cav3.1 and Cav 3.2 immunostaining measured by *histoscore* on normal skin, common and dysplastic nevi and melanoma samples**

TT-C isoform	Cav3.1 (p-value)	Cav3.2 (p-value)
Global differences 5-groups	<0.0001	<0.0001
NS vs ACMN	ns	<0.0001
NS vs DN	ns	<0.0001
NS vs pMM	ns	<0.0001
NS vs mMM	<0.01	<0.0001
ACMN vs DN	<0.05	ns
ACMN vs pMM	<0.01	ns
ACMN vs mMM	<0.0001	<0.0001
DN vs pMM	ns	ns
DN vs mMM	ns	<0.0001
pMM vs mMM	ns	<0.0001
Trend-test	<0.0001	<0.0001

TT-C (T-type channel); NS (epidermal melanocytes on normal skin); CAMN (common acquired melanocytic nevi); DN (dysplastic nevi); MM (melanoma) pMM (primary melanoma); mMM (metastatic melanoma). Kruskal-Wallis test with Post Hoc Dunn's Multiple Comparison Test was performed to study differences in the expression of TT-C isoforms in all skin groups. A trend test, using a linear model, was used to evaluate the progression in the Hs levels.

**SUPPLEMENTARY TABLE 5. Statistical comparison of mean Cav3.1 and Cav 3.2 immunostaining measured by *histoscore* on thin (Breslow ≤1mm) vs thick (Breslow >1 mm) primary melanoma tumors**

	All pMM	Breslow		Test
		≤ 1mm	>1mm	non-parametric
TT-C isoform	Mean (SD)	Mean (SD)	Mean (SD)	p-value
Cav3.1 (Hs)	34.45 (44.09)	33.68 (39.12)	48.33 (54.71)	<0.00001*
Cav 3.2 (Hs)	85.39 (90.24)	83.42 (78.25)	160.00 (72.85)	<0.00001*

TT-C (T-type channel); pMM (primary melanoma). Histoscore mean were analyzed by Mann-Whitney test. SD: Standard deviation

**SUPPLEMENTARY TABLE 6. Differential immunoexpression of Cav 3.1 and Cav 3.2 measured by *histoscore* according to primary melanoma subtype**

	All pMM	pMM subtypes					
		SSMM	SSMM ≤4 mm	SSMM >4mm	NM	ALM	LMM
TT-C isoform	Mean (SD)	Mean (SD)	Mean (SD)	Mean (SD)	Mean (SD)	Mean (SD)	Mean (SD)
<b>Cav3.1 (Hs)</b>	34.45 (44.09)	41.74 (55.51)	31.00 (42.94)	61.88 (71.48)	48.33 (50.31)	32.50 (41.44)	72.00 (32.59)
<b>Cav 3.2 (Hs)</b>	85.39 (90.24)	67.17 (59.43)	46.67 (51.48)	105.6 (54.77)	212.22 (28.95)	198.33 (51.93)	201.0 (30.71)

TT-C (T-type channel); pMM (primary melanoma), SSMM (superficial spreading malignant melanoma); NM (nodular melanoma); ALM (acral lentiginous melanoma); LMM (lentigo.malignant melanoma). SSMM have been also divided according Breslow thickness. SD: Standard deviation

**SUPPLEMENTARY TABLE 7. Statistical comparison of mean Cav3.1 and Cav 3.2 immunostaining measured by *histoscore* according to primary melanoma subtype**

TT-C isoform	Cav3.1 (p-value)	Cav3.2 (p-value)
Global differences 5-groups	0.07	<0.0001
SSMM≤ 4 vs SSMM > 4	ns	ns
SSMM≤ 4 vs NM	ns	<0.0001
SSMM≤ 4 vs ALM	ns	<0.0001
SSMM≤ 4 vs LMM	ns	<0.0001
SSMM> 4 vs NM	ns	<0.0001
SSMM> 4 vs ALM	ns	<0.05
SSMM> 4 vs LMM	ns	<0.05
NM vs ALM	ns	ns
NM vs LMM	ns	ns
ALM vs LMM	ns	ns

TT-Cs (T-type channel); pMM (primary melanoma), SSMM (superficial spreading malignant melanoma); NM (nodular melanoma); ALM (acral lentiginous melanoma); LMM (lentigo.malignant melanoma). SSMM have been also divided according to Breslow thickness. Kruskal-Wallis test with post Hoc Dunn's Multiple Comparison Test was performed to study differences in the expression of TT-Cs isoforms between pMM subtypes.